

RESEARCH

Succinate dehydrogenase variants in paraganglioma: why are B subunit variants ‘bad’?

Lucinda M Gruber¹, Steven N Hart² and Louis James Maher III³ ¹Division of Endocrinology, Mayo Clinic, Rochester, Minnesota, USA²Department of Computational Pathology and Artificial Intelligence, Mayo Clinic, Rochester, Minnesota, USA³Department of Biochemistry and Molecular Biology, Mayo Clinic, Rochester, Minnesota, USACorrespondence should be addressed to L J Maher: maher@mayo.edu

Abstract

Mutations that predispose to familial pheochromocytoma and paraganglioma include inherited variants in the four genes (*SDHA*, *SDHB*, *SDHC* and *SDHD*) encoding subunits of succinate dehydrogenase (SDH), an enzyme of the mitochondrial tricarboxylic acid cycle and complex II of the electron transport chain. In heterozygous variant carriers, somatic loss of heterozygosity is thought to result in tumorigenic accumulation of succinate and reactive oxygen species. Inexplicably, variants affecting the *SDHB* subunit predict worse clinical outcomes. Why? Here we consider two hypotheses. First, relative to *SDH* A, C and D subunits, the small *SDHB* subunit might be more intrinsically ‘fragile’ to missense mutations because of its relatively large fraction of amino acids contacting prosthetic groups and other *SDH* subunits. We show evidence that supports this hypothesis. Second, the natural pool of human *SDHB* variants might, by chance, be biased toward severe truncating variants and missense variants causing more disruptive amino acid substitutions. We tested this hypothesis by creating a database of known *SDH* variants and predicting their biochemical severities. Our data suggest that natural *SDHB* variants are more pathogenic. It is unclear if this bias is sufficient to explain clinical data. Other explanations include the possibility that *SDH* subcomplexes remaining after *SDHB* loss have unique tumorigenic gain-of-function characteristics, and/or that *SDHB* may have additional unknown tumor-suppressor functions.

Key Words

- ▶ succinate dehydrogenase
- ▶ paraganglioma
- ▶ pheochromocytoma
- ▶ missense variant
- ▶ pathogenicity

Endocrine Oncology
(2023) 3, e220093

Introduction

Pheochromocytoma and paraganglioma (PPGL) are rare neuroendocrine tumors (Pang *et al.* 2019, Botta *et al.* 2020). Different classes of driver mutations have been identified, leading to the designation of cluster 1 tumors (driven by defects that trigger a chronic hypoxic response), cluster 2 tumors (driven by mutations in *WNT* signaling pathways) and cluster 3 tumors (driven by hyperactive kinase signaling pathways) (Castro-Vega *et al.* 2015, Fishbein *et al.* 2017, Taieb & Pacak 2017, Pang *et al.* 2019). Cluster 1 tumors are particularly

fascinating because a sub-group is driven by inherited genetic variants in succinate dehydrogenase (SDH). This mitochondrial enzyme catalyzes a step of the tricarboxylic acid cycle and serves as complex II of the electron transport chain. SDH is comprised of four nuclear-encoded subunits, A, B, C and D (Fig. 1A). The SDH heterotetramer is found across all kingdoms of life and is highly conserved through evolution. According to the current hypotheses (Pang *et al.* 2019, Buffet *et al.* 2020), heterozygous carriers of a wildtype SDH subunit

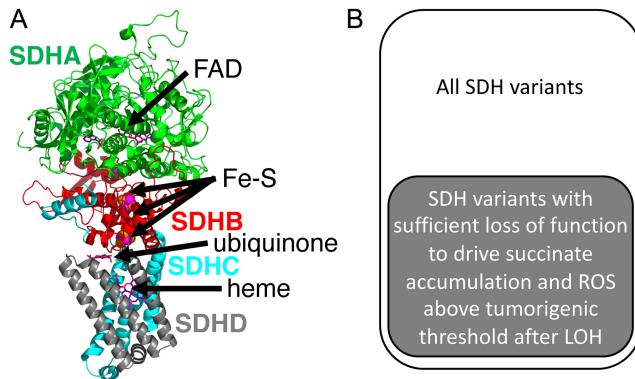


Figure 1
Approach to hypothesis test. (A) SDH subunit structure based on porcine complex 1Z0Y in pdb. (B) Operating hypothesis.

allele and a predisposing SDH variant subunit allele are asymptomatic but at risk for stochastic somatic loss of heterozygosity (LOH) removing the functional SDH subunit gene. When such LOH occurs in a susceptible tissue, PPGL may result. After LOH, deleterious genetic variants in any of the four SDH subunits or a crucial assembly factor (Buffet *et al.* 2020) presumably result in diminished (or zero) residual SDH activity with accumulation of tumorigenic levels of succinate and reactive oxygen species (ROS) (Selak *et al.* 2005, Smith *et al.* 2007, Liu *et al.* 2020). In the case of succinate accumulation, tumorigenesis is thought to result from the ability of succinate to poison dozens of cellular dioxygenase enzymes, including those responsible for marking HIF transcription factors for degradation in normoxia (Selak *et al.* 2005, Her & Maher 2015) and those responsible for epigenetic demethylation of histones and DNA (Smith *et al.* 2007, Letouze *et al.* 2013). There is evidence that synergy between chronic pseudohypoxic signaling and derangement of DNA methylation then drives tumorigenesis (Morin *et al.* 2020). ROS accumulation in SDH-loss cells reportedly results from iron overload (Liu *et al.* 2020), with the potential to drive reduction/oxidation (REDOX) reaction imbalance.

Our fundamental tumorigenesis model for this study is shown in Fig. 1B. We assume that SDH subunit variants inhibit SDH activity to different extents. After LOH, only a subset of variants are sufficiently biochemically severe to drive succinate and/or ROS accumulation above some tumorigenic threshold in susceptible neuroendocrine cells. We further assume that tumor penetrance, severity and metastasis are then dependent on the levels of accumulated succinate

and ROS, meaning that variants with less residual SDH activity are more pathogenic. By this reasoning, it is not prognostically adequate to note only which is the variant subunit, but it is necessary to consider the biochemical impact of the particular inherited variant on SDH activity. A related hypothetical model has also recently been proposed (Bayley & Devilee 2022).

Clinicians have long appreciated that PPGL in carriers of SDHB variants tend to present with a more aggressive clinical phenotype, including increased risk of metastatic disease (Andrews *et al.* 2018, Hescot *et al.* 2019, Lee *et al.* 2019, Muth *et al.* 2019, Rijken *et al.* 2019). More than 40% of SDHB variant carriers are reported to have developed PPGL by age 70 (Jochmanova *et al.* 2017, Rijken *et al.* 2019), and about 60% of the tumors have been reported to metastasize (Jochmanova *et al.* 2017). These values are substantially higher than for other SDHx variants, resulting in the adage that ‘B is bad’. The basis for this SDHB effect is unknown, and it persists as one of several paradoxes associated with PPGL. The result appears counterintuitive if biochemical severities of SDH variants are equally likely for different SDH subunits, as loss of function of any subunit would presumably inactivate the SDH complex.

Here, we consider possible biochemical and population genetic hypotheses to explain why ‘B is bad’. First, we explore the possibility that the SDHB subunit is intrinsically ‘fragile’ to missense variants, hypothesizing that SDHB has a relatively high density of amino acid residues that make essential contacts to other SDH subunits and to crucial iron–sulfur cluster prosthetic groups and their insertion cue residues. If the biochemical severity (i.e. non-conservative amino acid side chain character) of missense variants is comparable among SDH subunits, this SDHB ‘fragility’ would predict that random missense variants would be more likely to be deleterious for SDHB. In such a scenario, detection of an SDHB missense variant would imply greater biochemical severity and greater pathogenic probability and account for the ‘B is bad’ adage. Second, we explore the actual distribution of variant types (truncating vs missense variants) and predicted biochemical severity of missense variants among extant SDH subunit genes, hypothesizing that, by chance, more naturally occurring SDHB variants in the human population happen to have biochemically severe consequences than for other SDH subunits. Such a scenario would also explain why ‘B is bad’.

Materials and methods

SDH subunit interface area

Interface area (IA) between SDH subunits was calculated from the porcine x-ray crystal structure (pdb: 1ZOY (Sun *et al.* 2005)) by two methods. First, PyMOL (Version 2.0 Schrödinger, LLC) was used to determine the surface area (Å²) for each subunit and each combination of subunits (e.g. A–B interface, B–C interface, etc., as detailed in supplemental materials). For example, the interface surface area between subunits A and B (IA_{A,B}, in units of Å²) was calculated according to Equation 1:

$$IA_{A,B} = \frac{(SA_{subunits\ A+B}) - (SA_{subunit\ A} + SA_{subunit\ B})}{2} \quad (1)$$

where SA is surface area. The interface area was then divided by the total surface area for the subunit to give the percent of the subunit surface area involved in interface with other SDH subunits.

The proportion of interface for each SDH subunit was also calculated in terms of inter-subunit amino acid contacts using the Protein Contact Atlas resource (Kayikci *et al.* 2018) (<http://www.mrc-lmb.cam.ac.uk/pca/>) applied to pdb: 1ZOY. Dividing the sum of inter-subunit amino acid contacts by the total number of amino acids in each SDH subunit produced an interface contact per amino acid statistic for each subunit.

Essential molecular features for subunits

Essential molecular features (EMFs) of SDH were defined as flavin adenine dinucleotide (FAD), heme, ubiquinone (UBQ), Fe-S clusters, and the I/LYR residues of SDHB (tripeptides at positions 44–46 and 240–242 essential for placement of Fe-S clusters) (Saxena *et al.* 2015). The total number of amino acid contacts with EMF was determined for each SDH subunit using the Protein Contact Atlas (Kayikci *et al.* 2018) (<http://www.mrc-lmb.cam.ac.uk/pca/>) applied to pdb: 1ZOY. Dividing EMF contacts for each SDH subunit by the total number of amino acids in that subunit produced an EMF contact per amino acid statistic for each subunit.

SDH variant database

Four databases were used to compile a comprehensive collection of unique human SDH variants: (i) Genome Aggregation Database (gnomAD; <https://gnomad.org/>);

(ii) Leiden Open (Source) Variation Database (LOVD); Database (<https://www.lovd.nl/>); (iii) ClinVar (National Center for Biotechnology Information, <https://ncbi.nlm.nih.gov/clinvar/>); and (iv) Mayo Clinic Division of Endocrinology PPGL case database (Hamidi *et al.* 2017).

Truncating vs missense variants

Variants were categorized as truncating or missense. Truncating variants included variants introducing premature stop codons, altering splice acceptor/donor nucleotides, and/or frameshift mutations. Missense variants produce amino acid substitutions. Synonymous variants were not included in this analysis. Normalized truncation location was calculated as the affected amino acid position, divided by the total number of amino acids in the subunit, and reported as a percentage.

Prediction of missense variant biochemical severity

Two approaches were used to predict the biochemical severity of missense variants. First, an ad hoc impact score was calculated. The Protein Contact Atlas (<http://www.mrc-lmb.cam.ac.uk/pca/>) was applied to pdb: 1ZOY (Sun *et al.* 2005) to determine the proximity of each SDH missense variant to subunit interfaces and EMFs. An ad hoc biochemical severity score was based on the premise that amino acid substitutions are more likely to be disruptive to SDH activity if chemically nonconservative and to the extent that they occur in proximity to subunit interfaces and/or EMF. Ad hoc biochemical severity scores (larger score for more disruptive variants) were assigned as follows:

1. Direct contacts: score 3 if ≤25% of variant contacts involve an SDH subunit interface; score 4 if >25% of variant contacts involve an SDH subunit interface; score 8 if variant directly contacts an EMF (except score 1 for direct contact to heme where physiological function is debated).
2. Indirect contacts: score 1 if ≤25% of variant contacts involve an SDH subunit interface; score 2 if >25% of variant contacts involve an SDH subunit interface; score 2 if indirect contacts to EMF (except score 1 for indirect contact to heme).
3. The evolutionary conservation of the amino acid substitution (BLOSUM) was assigned using the Blocks Substitution Matrix (BLOSUM62 (Henikoff & Henikoff 1992)).

- An arbitrary base (B) weighted by the negative power of the BLOSUM score was created as the multiplier to account for the degree of conservation of the amino acid substitution. Here, the assigned value of B was 2.

The ad hoc biochemical severity score (I) was then calculated using these values according to Equation 2:

$$I = (Direct_{SI} + Indirect_{SI} + Direct_{EMF} + Indirect_{EMF}) * B^{(-BLOSUM)} \quad (2)$$

where subscript SI refers to subunit interface contact counts and subscript EMF to EMF contact counts. The supplemental materials include the SDH variant database and an interactive missense variant formula where the user can explore how the value of B (weighting of the contribution of amino acid side chain conservation) affects the ad hoc severity score.

The biochemical severity of missense variants was independently estimated according to evolutionary tolerance for amino acid substitutions using the Sorting Intolerant from Tolerant (SIFT) tool (Sim *et al.* 2012). Default program settings were used. In this case, lower scores predict more disruptive variants. It should be noted that, like the ad hoc severity score calculated in this work, SIFT also considers the BLOSUM matrix. The two methods are thus not completely independent.

Results

We set out to explore the possibility that SDHB variants are more penetrant and likely to drive malignancy because the average SDHB variant is more biochemically severe, resulting in a greater loss of SDH activity and greater accumulation of succinate and/or ROS. We considered two hypotheses. First, we studied intrinsic features of the SDHB subunit that might make random amino acid substitutions more damaging to SDH activity compared to random substitutions in the A, C or D subunits. Second, we studied a collection of actual human SDH subunit variants to test the possibility that, by chance, actual SDHB variants in the population tend to be more biochemically severe.

Intrinsic fragility of the SDHB subunit

Inspection of the porcine SDH crystal structure (Fig. 1A) reveals the tertiary and quaternary structure of the complex and distribution of prosthetic groups, including FAD (SDHA), three Fe-S clusters (SDHB) and

UBQ and heme groups (SDHC and SDHD). It is evident that SDHB is small and sandwiched between the other three subunits, suggesting that its relative fraction of contact surface area is high. This, together with conserved amino acids in SDHB that form Fe-S clusters and two I/LYR tripeptides of SDHB required for cueing this process (Saxena *et al.* 2015), suggests that SDHB might be unique among SDH subunits in its density of sensitive amino acids contacting interfaces and EMFs. This concept is depicted schematically in Fig. 2.

We confirmed this intuition by two kinds of calculations based on the SDH structure (Table 1). For each SDH subunit (Table 1, column 1), we used molecular modeling (supplemental methods, see section on supplementary materials given at the end of this article) to calculate the surface area (Table 1, column 2), interface surface area (Table 1, column 3) and fractional interface surface area (Table 1, column 4). These calculations reveal that 40% of SDHB surface area forms interfaces with other SDH subunits, compared to only 28% for the C and D subunits, and only 13% for the large SDHA subunit. This implies that random missense variants are

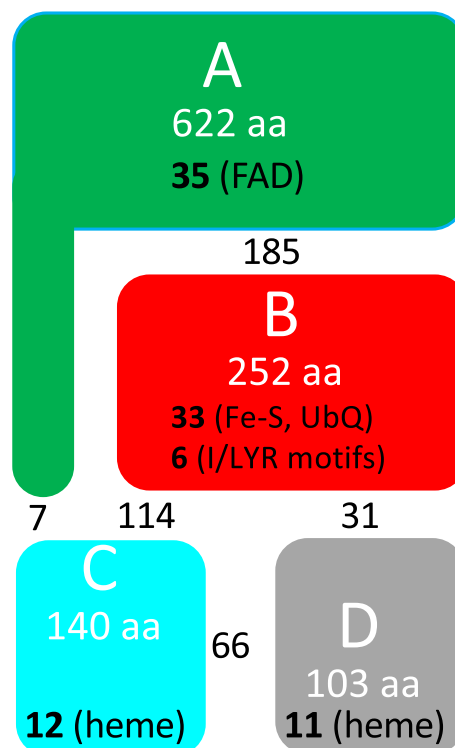


Figure 2

Schematic illustration of SDH subunits and amino acid contacts. Mature SDH subunit size (amino acids) is indicated along with contacts with interfaces and prosthetic group (FAD, Fe-S clusters, heme) or prosthetic group insertion signals (I/LYR motifs) from Protein Contact Atlas, based on porcine complex 1ZOY in pdb.

Table 1 SDH subunit structural features.^a

SDH subunit (L) ^b	Surface (Å ²)	Interface surface	Fraction interface	Interface contacts, S (S/L)	EMF contacts, F (F/L)	Total contacts, S+F ((S+F)/L)
A (622)	22,383	2795	0.13	192 (0.31)	35 ^c (0.06)	227 (0.36)
B (252)	13,222	5247	0.40	330 (1.31)	39^d (0.15)	369 (1.46)
C (140)	11,445	3226	0.28	187 (1.34)	12 ^e (0.09)	199 (1.42)
D (103)	7618	2116	0.28	97 (0.94)	11 ^f (0.11)	108 (1.05)

Bold values indicate greatest value in column.

^aCalculated from data in PDB:1ZOY using Pymol and Protein Contact Atlas; ^bMature subunit length in amino acids, based on the following encoded lengths and mitochondrial targeting peptides: SDHA, 664, 1–42; SDHB, 280, 1–28; SDHC, 169, 1–29; SDHD, 159, 1–56.; ^cContacts involving FAD; ^dContacts involving iron–sulfur clusters and ubiquinone (33), and I/LRY motifs (6); ^eContacts with heme; ^fContacts with heme.

more likely to be biochemically deleterious in SDHB than the other SDH subunits.

We then employed the Protein Contact Atlas resource (Kayikci *et al.* 2018) to compare the numbers of SDH subunit amino acids that make direct and indirect contacts with other subunits (Table 1, column 5) and with EMFs (Table 1, column 6). Interestingly, while the total number of interface contacts is highest for SDHB, the proportion of subunit amino acids relative to subunit chain length is actually highest for SDHC (Table 1, column 5). The number and proportion of EMF contacts are highest for SDHB (Table 1, column, 6). Both total contacts and their relative proportion to subunit size are also the highest for SDHB, with SDHC slightly lower (Table 1, column 7). We conclude that the structure of the SDH complex implies that SDHB is somewhat more ‘fragile’ than other SDH subunits: random amino acid substitutions in SDHB are more likely to be deleterious simply because of SDHB structure.

SDHB fragility estimated from evolutionary conservation

The SIFT tool (Sim *et al.* 2012) also offers an objective approach to compare SDH subunits for the number and proportion of amino acid positions predicted to be intolerant to substitution based on evolutionary conservation. We estimated SDH subunit fragility by calculating the number of amino acid positions showing evolutionary tolerance for four or fewer amino acid substitutions (Table 2, column 3) and expressed this number as a fraction of all subunit amino acids well-aligned over evolution (Table 2, column 4). SDHB shows the greatest fraction of such intolerant amino acid residues. We conclude from evolutionary conservation that SDHB is the most sensitive to nonconservative amino acid variants, with other SDH subunits being less fragile.

Table 2 SDH subunit fragility based on SIFT.

SDH subunit (L) ^a	Aligned positions ^b (P)	Positions tolerating four or fewer substitutions (S)	Fraction (P/S)
A (622)	475	246	0.52
B (252)	187	106	0.57
C (140)	100	38	0.38
D (103)	93	49	0.53

Bold indicates greatest value in column.

^aMature subunit length in amino acids; ^bNumber of amino acid positions with SIFT alignment score of 1.0.

Estimating biochemical severities of actual SDH subunit variants in the actual human population

We also wished to test the hypothesis that actual SDHB variants in the human population are, by chance, more biochemically deleterious. We assembled a composite SDH variant database combining records from gnomAD, clinvar, LOVD, and Mayo Clinic (see the ‘Materials and methods’ section). As shown in Table 3, this database (Supplemental spreadsheet) identifies 2171 unique SDH variants, including variants in SDHA (811, 37%), SDHB (668, 31%), SDHC (306, 14%) and SDHD (386, 18%). These SDH variants were identified in a pool of 214,805 total SDH variant genomes, distributed as: SDHA (83,641, 38.9%), SDHB (6536, 3.0%), SDHC (2724, 1.3%) and SDHD (121,904, 56.8%). The numbers of unique SDH variants per subunit coding region length were 1.22 (SDHA), 2.39 (SDHB), 1.81 (SDHC) and 2.43 (SDHD).

Truncating variants

We assumed that truncating variants are, on average, more biochemically deleterious than missense variants. We therefore compared the fraction of unique truncating SDH variants for each SDH subunit (Table 3, column 3). Unique truncating variants were less common overall than missense variants, and the fraction of unique truncating variants is slightly higher for SDHD (46%)

Table 3 Truncating vs missense SDH variants.

SDH subunit	Variant type	n (%) ^a
A	Total	83,641 (100%, 38.9%)
	Missense	83,344 (99.6%, 38.8%)
	Truncating	297 (0.4%, 0.14%)
B	Total	6536 (100%, 3.0%)
	Missense	6133 (93.8%, 2.9%)
	Truncating	403 (6.2% , 0.19%)
C	Total	2724 (100%, 1.3%)
	Missense	2572 (94.4%, 1.2%)
	Truncating	152 (5.6%, 0.07%)
D	Total	121,904 (100%, 56.8%)
	Missense	121,681 (99.8%, 56.6%)
	Truncating	223 (0.2%, 0.1%)

Bold indicates highest truncating percentage in column

^an, variants as number (percent for subunit, percent overall) of total genomes (214,805).

than SDHB (45%). To understand apparent prognostic risk for truncating variants in any SDH subunit, we calculated the fraction of truncating variants in all sequenced genomes in the database. This calculation indicates that an individual selected at random from the population of all individuals with SDHB variants has the highest likelihood of carrying a truncating variant (6.2%, **Table 3**, column 3), with SDHC truncating variant prevalence being slightly lower (5.6%).

Missense variants

We sought to predict the biochemical severities of unique SDH missense variants and the distribution of these predicted biochemical severities among SDH subunits. For this analysis, we applied two methods to estimate the biochemical severity of missense variants according to Equations 3–5.

First, we developed an ad hoc scoring algorithm (see ‘Materials and methods’) that leveraged the known porcine SDH x-ray crystal structure ([Sun *et al.* 2005](#)), the Protein Contacts Atlas tool ([Kayikci *et al.* 2018](#)) and the BLOSUM62 matrix ([Henikoff & Henikoff 1992](#)) that quantitatively evaluates evolutionary conservation of amino acid side chain biochemical properties. The parameters of the ad hoc scoring function (‘Materials and methods’ section, Equation 2, supplemental spreadsheet) can be adjusted for comparative purposes. The ad hoc scoring function was applied to all SDH missense variants in our database. Results are shown in column 2 of **Table 4**. Interestingly, this approach predicts that unique missense SDHB variants in the human population are more deleterious than missense variants in other SDH subunits.

Second, we applied the well-established SIFT algorithm to score missense variants for biochemical severity based on evolutionary conservation. The results are shown in column 3 of **Table 4**. Interestingly, the SIFT algorithm also predicts that the unique SDHB missense variants are more biochemically severe than other SDH subunit missense variants (**Table 4**, column 3). In summary, two pathogenicity prediction methods predict that the known unique missense variants in SDHB are more severe than the missense variants in other SDH subunits.

Discussion

Clinicians have been taught to assign familial PPGL risk on the basis of the involved SDH subunit. This is an obvious oversimplification because individual variants differ in biochemical severity. In this study, we assume that the degree of SDHx variant pathogenicity (PPGL tumorigenicity, aggressiveness and metastasis) is determined by the biochemical effect on SDH activity revealed after LOH – the lower the residual SDH activity, the greater the pathogenicity of the variant. Our work extends important prior studies that have connected SDH variant genotype to phenotype in PPGL ([Ricketts *et al.* 2010](#), [Saxena *et al.* 2015](#), [Jochmanova *et al.* 2017](#), [Andrews *et al.* 2018](#), [Benn *et al.* 2018](#), [Hescot *et al.* 2019](#), [Lee *et al.* 2019](#), [Muth *et al.* 2019](#), [Bayley *et al.* 2020](#)). Interestingly, a previous study monitored metabolites in tumor specimens representing 24 SDHB mutants, 2 SDHC mutants and 19 SDHD mutants ([Richter *et al.* 2014](#)). Individual genotypes are not presented for most of these cases, preventing prediction of variant pathogenicity. The metabolite results nonetheless tend to support the notion of intrinsic SDHB fragility: while levels of succinate accumulation are similar between different SDHx mutations, levels of fumarate (the product of the SDH-catalyzed reaction)

Table 4 Ad hoc and SIFT mean scores for unique missense SDH variants

SDH subunit	Mean score unweighted	
	Ad hoc ^a	SIFT ^b
A	3.2	0.18
B	15.0	0.16
C	10.3	0.24
D	10.0	0.40

Bold indicates the most deleterious mean in column.

^aAd hoc score: by convention, higher score indicates more deleterious;

^bSIFT score: by convention, lower score indicates more deleterious.

were lower for SDHB mutant tumors than for SDHC and SDHD mutants.

'B is bad': SDHB fragility?

We show that intrinsic structural characteristics of the SDH enzyme subunits imply that random missense mutations are more likely to be biochemically deleterious in the small SDHB subunit. SDHB is fragile because of its relatively high density of amino acid residues contacting other subunits and EMFs. SDHB fragility is demonstrated by surface area calculations, contact inventories, and greater predicted intolerance to non-conserved amino acid substitutions based on evolutionary alignments. These observations support the hypothesis that random SDHB missense variants are more penetrant and malignant simply because they are more disruptive to SDH activity, resulting in higher succinate and ROS accumulation than missense variants in other SDH subunits. What remains unclear is whether this differential SDHB fragility (Table 1 and Table 2) is sufficient to explain the striking excess clinical risk for PPGL patients carrying SDHB variants.

'B is bad': population distribution of actual SDH variants?

We created a database of actual SDHx variants to investigate the distribution of predicted variant biochemical severity. The fraction of truncating variants is marginally higher for SDHB than SDHC for all sequenced genomes (Table 3). When considering patients with clinical disease (PPGL), a prior study also showed truncating variants in SDHB were most common followed by missense variant in SDHB and truncating variants in SDHD (Bayley *et al.* 2020). Thus, these results tend to support a hypothesis that SDHB variants in the human population are, by chance, more likely to be severe truncating variants. However, the difference between SDHB and SDHC is not large, again making it questionable whether this statistical effect accounts for striking clinical differences.

In addition to these findings, we estimated the biochemical severity of each unique SDHx missense variant in our database. Both ad hoc and conventional scoring methods were used, predicting the unique SDHB missense variants in the human population to be more biochemically severe than other SDH subunit variants (Table 4).

These data related to structural and statistical explanations for the uniquely pathogenic impact of

SDHB variants on PPGL outcomes marginally support the original hypotheses. We show several lines of structural evidence that the SDHB subunit is intrinsically fragile to amino acid substitution variants relative to other SDH subunits. Based on an actual database of SDH variants, we also show that unique SDHB missense variants in the population are marginally more likely to be severe truncation mutations (Table 3). Unique SDHB missense variants in the human gene pool are also predicted to be marginally more deleterious. It remains questionable whether the observed trends in SDHB variant biochemical severity are sufficient to explain the striking clinical severity of SDHB variants.

Future efforts could be directed to estimate the prevalence of all unique truncating and missense SDH variants in the human population in order to test the additional hypothesis that more deleterious SDHB variants happen to be, by chance, overrepresented relative to deleterious variants in other SDH subunits.

'B is bad': alternative explanations

Beyond hypothetical structural and statistical explanations for SDHB variant penetrance and malignancy proposed here, there are at least two obvious alternative explanations for the special negative consequences associated with SDHB variants. The first possibility is that loss or dysfunction of the SDHB subunit leaves a uniquely pathogenic configuration of residual SDH polypeptides. For example, it has been reported that knockdown of SDHB or SDHC subunits yields a persistent complex containing SDHA and accessory factors (CII_{low}) (Bezawork-Geleta *et al.* 2018). In contrast, knockdown of SDHA leads to degradation of both SDHB and SDHC (and presumably SDHD). There is also evidence in yeast that SDH1 (the yeast ortholog of SDHA) persists upon loss of SDH2 (the yeast ortholog of SDHB) (Smith *et al.* 2007). Both of these results suggest the possibility that the residual SDHA subunit might result in pathogenic consequences that would differentiate SDHA loss from variants in other subunits. However, it is unclear how rogue residual SDHA activity would explain the particular pathogenicity of SDHB loss. It has long been suggested that loss of any other SDH subunit destabilizes SDHB (Gill *et al.* 2010), suggesting that loss of SDHB, C or D should all generate the same residual SDHA (and CII_{low}) proteins. It remains possible that the activities of residual SDH subunits are subtly different for cases where SDHB is never assembled vs cases where it is assembled but then degraded.

Another possibility is that SDHB performs an additional unknown tumor-suppressor function beyond its role as an SDH subunit. Although such a special role for SDHB has not been detected in *S. cerevisiae*, other aspects of SDH function in budding yeast are illuminating. For example, the yeast SDHC ortholog (*SDH3*) has been shown to play an unexpected moonlighting role as part of the yeast TIM22 protein translocase of the mitochondrial inner membrane (Gebert *et al.* 2011). Likewise, the *S. cerevisiae* *SDH3* and *SDH4* genes both have expressed paralogs, *SHH3* and *SHH4*, believed to have arisen by genome duplication. These proteins may partially substitute for one another, complicating yeast SDH genetics. These insights from budding yeast serve as reminders that unexpected human SDH genetic and biochemical complexities are possible. Exploring these fascinating possibilities will be an important goal for future research.

Supplementary materials

This is linked to the online version of the paper at <https://doi.org/10.1530/EO-22-0093>.

Declaration of interest

The authors believe that there is no conflict of interest that could be perceived as prejudicing the impartiality of the research reported.

Funding

This work was supported by Mayo Clinic and a generous grant from the Paradifference Foundation.

Ethics statement

The institutional review board at Mayo Clinic in Rochester, MN, approved this study. As a retrospective review, direct re-consent was not obtained from patients. We followed ethical guidelines outlined by the Declaration of Helsinki and the state of Minnesota. Some findings were presented at the Endocrine Society Conference 2021 as a poster presentation. The interim abstract was published in the *Journal of the Endocrine Society*, Volume 5, Issue Supplement_1, April–May 2021, Pages A71–A72, <https://doi.org/10.1210/jendso/bvab048.144>

Author contribution statement

LG conceived the study, assembled the database, performed analyses and co-wrote the paper. SH consulted on the study approach and edited the paper. LJM conceived the study, performed analyses and co-wrote the paper.

Acknowledgements

The authors appreciate the expertise of Dragana Milosevic in the Department of Laboratory Medicine and Pathology and Irina Bancos in the Division of Endocrinology, Mayo Clinic, Rochester, MN.

References

- Andrews KA, Ascher DB, Pires DEV, Barnes DR, Vialard L, Casey RT, Bradshaw N, Adlard J, Aylwin S, Brennan P, *et al.* 2018 Tumour risks and genotype-phenotype correlations associated with germline variants in succinate dehydrogenase subunit genes SDHB, SDHC and SDHD. *Journal of Medical Genetics* **55** 384–394. (<https://doi.org/10.1136/jmedgenet-2017-105127>)
- Bayley JP, Bausch B, Rijken JA, Van Hulsteijn LT, Jansen JC, Ascher D, Pires DEV, Hes FJ, Hensen EF, Corssmit EPM, *et al.* 2020 Variant type is associated with disease characteristics in SDHB, SDHC and SDHD-linked pheochromocytoma-paraganglioma. *Journal of Medical Genetics* **57** 96–103. (<https://doi.org/10.1136/jmedgenet-2019-106214>)
- Bayley JP & Devilee P 2022 Hypothesis: why different types of SDH gene variants cause divergent tumor phenotypes. *Genes (Basel)* **13** 1025. (<https://doi.org/10.3390/genes13061025>)
- Benn DE, Zhu Y, Andrews KA, Wilding M, Duncan EL, Dwight T, Tothill RW, Burgess J, Crook A, Gill AJ, *et al.* 2018 Bayesian approach to determining penetrance of pathogenic SDH variants. *Journal of Medical Genetics* **55** 729–734. (<https://doi.org/10.1136/jmedgenet-2018-105427>)
- Bezawork-Geleta A, Wen H, Dong L, Yan B, Vider J, Boukalova S, Krobova L, Vanova K, Zobalova R, Sobol M, *et al.* 2018 Alternative assembly of respiratory complex II connects energy stress to metabolic checkpoints. *Nature Communications* **9** 2221. (<https://doi.org/10.1038/s41467-018-04603-z>)
- Botta L, Gatta G, Trama A, Bernasconi A, Sharon E, Capocaccia R, Mariotto AB & RARECAREnet working group 2020 Incidence and survival of rare cancers in the US and Europe. *Cancer Medicine* **9** 5632–5642. (<https://doi.org/10.1002/cam4.3137>)
- Buffet A, Burnichon N, Favier J & Gimenez-Roqueplo AP 2020 An overview of 20 years of genetic studies in pheochromocytoma and paraganglioma. *Best Practice and Research. Clinical Endocrinology and Metabolism* **34** 101416. (<https://doi.org/10.1016/j.beem.2020.101416>)
- Castro-Vega LJ, Letouze E, Burnichon N, Buffet A, Disderot PH, Khalifa E, Lorient C, Elarouci N, Morin A, Menara M, *et al.* 2015 Multi-omics analysis defines core genomic alterations in pheochromocytomas and paragangliomas. *Nature Communications* **6** 6044. (<https://doi.org/10.1038/ncomms7044>)
- Fishbein L, Leshchiner I, Walter V, Danilova L, Robertson AG, Johnson AR, Lichtenberg TM, Murray BA, Ghayee HK, Else T, *et al.* 2017 Comprehensive Molecular Characterization of Pheochromocytoma and Paraganglioma. *Cancer Cell* **31** 181–193. (<https://doi.org/10.1016/j.ccell.2017.01.001>)
- Gebert N, Gebert M, Oeljeklaus S, Von Der Malsburg K, Stroud DA, Kulawiak B, Wirth C, Zahedi RP, Dolezal P, Wiese S, *et al.* 2011 Dual function of Sdh3 in the respiratory chain and TIM22 protein translocase of the mitochondrial inner membrane. *Molecular Cell* **44** 811–818. (<https://doi.org/10.1016/j.molcel.2011.09.025>)
- Gill AJ, Benn DE, Chou A, Clarkson A, Muljono A, Meyer-Rochow GY, Richardson AL, Sidhu SB, Robinson BG & Clifton-Bligh RJ 2010 Immunohistochemistry for SDHB triages genetic testing of SDHB, SDHC, and SDHD in paraganglioma-pheochromocytoma syndromes. *Human Pathology* **41** 805–814. (<https://doi.org/10.1016/j.humpath.2009.12.005>)
- Hamidi O, Young WF, Iniguez-Ariza NM, Kittah NE, Gruber L, Bancos C, Tamhane S & Bancos I 2017 Malignant pheochromocytoma and paraganglioma: 272 patients over 55 years. *Journal of Clinical Endocrinology and Metabolism* **102** 3296–3305. (<https://doi.org/10.1210/jc.2017-00992>)
- Henikoff S & Henikoff JG 1992 Amino acid substitution matrices from protein blocks. *PNAS* **89** 10915–10919. (<https://doi.org/10.1073/pnas.89.22.10915>)
- Her YF & Maher LJ 2015 Succinate dehydrogenase loss in familial paraganglioma: biochemistry, genetics, and epigenetics. *International Journal of Endocrinology* **2015** 296167. (<https://doi.org/10.1155/2015/296167>)

- Hescot S, Curras-Freixes M, Deutschbein T, Van Berkel A, Vezzosi D, Amar L, De La Fouchardière C, Valdes N, Riccardi F, Do Cao C, *et al.* 2019 Prognosis of malignant pheochromocytoma and paraganglioma (MAPP-Prono study): a European network for the study of adrenal tumors retrospective study. *Journal of Clinical Endocrinology and Metabolism* **104** 2367–2374. (<https://doi.org/10.1210/jc.2018-01968>)
- Jochmanova I, Wolf KI, King KS, Nambuba J, Wesley R, Martucci V, Raygada M, Adams KT, Prodanov T, Fojo AT, *et al.* 2017 SDHB-related pheochromocytoma and paraganglioma penetrance and genotype-phenotype correlations. *Journal of Cancer Research and Clinical Oncology* **143** 1421–1435. (<https://doi.org/10.1007/s00432-017-2397-3>)
- Kayikci M, Venkatakrishnan AJ, Scott-Brown J, Ravarani CNJ, Flock T & Babu MM 2018 Visualization and analysis of non-covalent contacts using the Protein Contacts Atlas. *Nature Structural and Molecular Biology* **25** 185–194. (<https://doi.org/10.1038/s41594-017-0019-z>)
- Lee H, Jeong S, Yu Y, Kang J, Sun H, Rhee J-K & Kim YH 2019. Risk of metastatic pheochromocytoma and paraganglioma in SDHx mutation carriers: a systematic review and updated meta-analysis. *Journal of Medical Genetics* **57** 217–225. (<https://doi.org/10.1136/jmedgenet-2019-106324>)
- Letouze E, Martinelli C, Loriot C, Burnichon N, Abermil N, Ottolenghi C, Janin M, Menara M, Nguyen AT, Benit P, *et al.* 2013 SDH mutations establish a hypermethylator phenotype in paraganglioma. *Cancer Cell* **23** 739–752. (<https://doi.org/10.1016/j.ccr.2013.04.018>)
- Liu Y, Pang Y, Zhu B, Uher O, Caisova V, Huynh TT, Taieb D, Hadrava Vanova K, Ghayee HK, Neuzil J, *et al.* 2020 Therapeutic targeting of SDHB-mutated pheochromocytoma/paraganglioma with pharmacologic ascorbic acid. *Clinical Cancer Research* **26** 3868–3880. (<https://doi.org/10.1158/1078-0432.CCR-19-2335>)
- Morin A, Goncalves J, Moog S, Castro-Vega LJ, Job S, Buffet A, Fontenille MJ, Woszczyk J, Gimenez-Roqueplo AP, Letouze E, *et al.* 2020 TET-mediated hypermethylation primes SDH-deficient cells for HIF2 α -driven mesenchymal transition. *Cell Reports* **30** 4551–4566. e7. (<https://doi.org/10.1016/j.celrep.2020.03.022>)
- Muth A, Crona J, Gimm O, Elmgren A, Filipsson K, Stenmark Askmalin M, Sandstedt J, Tengvar M & Tham E 2019 Genetic testing and surveillance guidelines in hereditary pheochromocytoma and paraganglioma. *Journal of Internal Medicine* **285** 187–204. (<https://doi.org/10.1111/joim.12869>)
- Pang Y, Liu Y, Pacak K & Yang C 2019 Pheochromocytomas and paragangliomas: from genetic diversity to targeted therapies. *Cancers (Basel)* **11** 436. (<https://doi.org/10.3390/cancers11040436>)
- Richter S, Peitzsch M, Rapizzi E, Lenders JW, Qin N, De Cubas AA, Schiavi F, Rao JU, Beuschlein F, Quinkler M, *et al.* 2014 Krebs cycle metabolite profiling for identification and stratification of pheochromocytomas/paragangliomas due to succinate dehydrogenase deficiency. *Journal of Clinical Endocrinology and Metabolism* **99** 3903–3911. (<https://doi.org/10.1210/jc.2014-2151>)
- Ricketts CJ, Forman JR, Rattenberry E, Bradshaw N, Laloo F, Izatt L, Cole TR, Armstrong R, Kumar VK, Morrison PJ, *et al.* 2010 Tumor risks and genotype-phenotype-proteotype analysis in 358 patients with germline mutations in SDHB and SDHD. *Human Mutation* **31** 41–51. (<https://doi.org/10.1002/humu.21136>)
- Rijken JA, Van Hulsteijn LT, Dekkers OM, Niemeijer ND, Leemans CR, Eijkelenkamp K, Van Der Horst-Schrivers ANA, Kerstens MN, Van Berkel A, Timmers HJLM, *et al.* 2019 Increased mortality in SDHB but not in SDHD pathogenic variant carriers. *Cancers (Basel)* **11** 103. (<https://doi.org/10.3390/cancers11010103>)
- Saxena N, Maio N, Crooks DR, Ricketts CJ, Yang Y, Wei MH, Fan TWM, Lane AN, Sourbier C, Singh A, *et al.* 2015 SDHB-deficient cancers: the role of mutations that impair iron sulfur cluster delivery. *Journal of the National Cancer Institute* **108** djv287–djv211. (<https://doi.org/10.1093/jnci/djv287>)
- Selak MA, Armour SM, Mackenzie ED, Boulahbel H, Watson DG, Mansfield KD, Pan Y, Simon MC, Thompson CB & Gottlieb E 2005 Succinate links TCA cycle dysfunction to oncogenesis by inhibiting HIF- α prolyl hydroxylase. *Cancer Cell* **7** 77–85. (<https://doi.org/10.1016/j.ccr.2004.11.022>)
- Sim NL, Kumar P, Hu J, Henikoff S, Schneider G & Ng PC 2012 SIFT web server: predicting effects of amino acid substitutions on proteins. *Nucleic Acids Research* **40** W452–W457. (<https://doi.org/10.1093/nar/gks539>)
- Smith EH, Janknecht R & Maher LJ, 3RD 2007 Succinate inhibition of α -ketoglutarate-dependent enzymes in a yeast model of paraganglioma. *Human Molecular Genetics* **16** 3136–3148. (<https://doi.org/10.1093/hmg/ddm275>)
- Sun F, Huo X, Zhai Y, Wang A, Xu J, Su D, Bartlam M & Rao Z 2005 Crystal structure of mitochondrial respiratory membrane protein complex II. *Cell* **121** 1043–1057. (<https://doi.org/10.1016/j.cell.2005.05.025>)
- Taieb D & Pacak K 2017 New insights into the nuclear imaging phenotypes of Cluster 1 pheochromocytoma and paraganglioma. *Trends in Endocrinology and Metabolism* **28** 807–817. (<https://doi.org/10.1016/j.tem.2017.08.001>)

Received 8 February 2023

Accepted 13 February 2023

Available online 14 February 2023

Version of Record published 29 March 2023